Viral Inhibition Studies on Sulfated Lignin, a Chemically Modified Biopolymer and a Potential Mimic of Heparan Sulfate

Arjun Raghuraman,[†] Vaibhav Tiwari,[‡] Qian Zhao,[§] Deepak Shukla,[‡] Asim K. Debnath,[§] and Umesh R. Desai*,[†]

Department of Medicinal Chemistry and Institute for Structural Biology and Drug Discovery, Virginia Commonwealth University, 410 North 12th Street, No. 542, Richmond, Virginia 23298, Departments of Ophthalmology and Visual Sciences, and Microbiology and Immunology, University of Illinois at Chicago, Chicago, Illinois 60612, and Lindsley F. Kimball Research Institute, New York Blood Center, New York, New York 10021

Received February 9, 2007
Revised Manuscript Received March 12, 2007

Introduction

Growing evidence suggests that heparan sulfate (HS), a proteoglycan present ubiquitously on nearly all cells, plays an important role in the initial attachment of enveloped viruses to target cells.[1−6] For example, herpes simplex virus (HSV) interaction with target cells involves cell surface HS interacting with several viral envelope proteins, especially glycoproteins gB, gC, and gD.[7−10] Likewise, gp120 and Tat of human immunodeficiency virus-1 (HIV-1) bind to HS to mediate the internalization of the virus.[11−13]

Glycosaminoglycan HS is a 1→4-linked linear polysaccharide of glucosamine (GlcN*p*) and glucuronic acid (GlcA*p*) residues, in which the majority of GlcN*p* residues are N-acetylated.[14,15] In addition, epimerization of some GlcA*p* residues to iduronic acid (IdoA*p*) and sulfation at the 2-, 3-, or 6-positions of GlcN*p* and 2-position of IdoA*p* introduce significant structural complexity and diversity in the HS biopolymer. Despite these large number of sequences, individual protein−HS interactions may involve specific binding sequences, as illustrated by the HS−gD interaction of HSV-1, which appears to be mediated by a rare 3-O-sulfated GlcN*p* residue.[8,10,16] Similar structural specificity has not yet been shown for HIV; however, size selectivity is apparent.[13,17]

Several sulfated carbohydrate including heparin, dextran sulfate, fucoidans, and sulfated galactans have been found to inhibit HSV and HIV because of their structural similarity to HS.[17−22] Recent studies on sulfated derivatives of *E. coli* K5 polysaccharides demonstrate good HIV-1 Tat protein antagonist activity.[23] Thus, we reasoned that sulfated non-polysaccharide scaffolds should also exhibit viral antagonist activity, similar to that displayed by the sulfated polysaccharides. A potential advantage with sulfated non-polysaccharide molecules would be their relatively easy chemical or chemo−enzymatic synthesis.

Our initial attempt to derive small sulfated non-saccharide molecules as viral antagonists led to the serendipitous discovery of a biological macromolecule that was found to inhibit HSV-1 entry into cells.[24] Elucidation of the structure of the active principle demonstrated it to be a sulfated derivative of lignin, a polymer made up of repeating phenylpropanoid units.[24] Lignin is abundantly available in nature, especially from plants and vegetables, and is a complex, heterogeneous organic scaffold, which is radically different from the polysaccharide backbone of HS.[25,26] In this note, we characterize the HSV-1, HSV-2, and HIV-1 inhibition and cytotoxic properties of lignin sulfate (LS) and demonstrate using comparative molecular modeling that certain structural features present in this interesting biopolymer may mimic HS structures, thus providing a basis for the observed viral inhibition property.

Experimental Methods

Chemicals, Cells, and Viruses. Lignin sulfate and morin sulfate (MoS) were prepared as described earlier.[24] β-Galactosidase substrate, *o*-nitrophenyl β-D-galactopyranoside (ONPG), was from Pierce (Rockford, IL). High-purity water, obtained from NERL Diagnostics (RI), was used in all experiments. Dr. Patricia Spear (Northwestern University) provided HeLa cells and the HSV reporter viruses listed here. HSV-1 and HSV-2 virus strains carrying the *lacZ* gene of *E. coli* and capable of expressing β-galactosidase as a reporter of entry included HSV-1(KOS) gL86 and HSV-2(333).[27,28] MT-2 cells, HIV-1_{IIIB}-infected H9 cells (H9/HIV-1_{IIIB}), and the HIV-1_{IIIB} isolate were obtained from the NIH AIDS Research and Reference Reagent Program.

HSV-1 and HSV-2 Virus Infection Assay. Assays for infection of cells were based on quantitation of β-galactosidase expressed by the mutant HSV viral genome containing the *lacZ* gene, as described earlier.[8,10] HeLa cells were grown in 96-well tissue culture dishes ($2-4 \times 10^4$ cells/well), washed after 16 h of growth, and exposed to 10 plaque-forming units (PFU)/cell of the HSV virus in 50 μL of phosphate-buffered saline (PBS) containing glucose and 1% calf serum (PBS-G-CS) for 6 h at 37 °C. To test for inhibitory activity, the sulfated compounds were simultaneously added to this 50 μL medium in varying amounts ranging from 0.2 μg to 1.6 ng. Following incubation, the cells were solubilized in 100 μL of PBS containing 0.5% NP-40 and 10 mM ONPG. The initial rate of hydrolysis of the substrate was monitored spectrophotometrically at 410 nm, which corresponds to the concentration of the β-galactosidase within HeLa K-1 cell. The initial rate of hydrolysis of the substrate in the absence of any added sulfated molecule formed the control and assigned a value of 100% HSV infection. Assays were performed in duplicate, and the mean value was used for calculation of IC_{50}, the concentration of inhibitor that reduces HSV infection by 50%.

HIV-1-Mediated Cell Fusion and p24 Assays. For detection of inhibition of HIV-1-mediated cell fusion, a dye transfer assay was used, as previously described.[29] Briefly, H9/HIV-1_{IIIB} cells were labeled with a fluorescent reagent, 2′,7′-bis(2-carboxyethyl)-5(and 6)-carboxyfluorescein acetoxyethyl ester (BCECF-AM, Molecular Probes, Inc., Eugene, OR) and then incubated with MT-2 cells (ratio = 1:10) in 96-well plates at 37 °C for 2 h in the presence or absence of the LS samples. The fused and unfused BCECF-labeled HIV-1-infected cells were counted under an inverted fluorescence microscope (Zeiss, Germany) with an eyepiece micrometer disk. The percentage of inhibition of cell fusion and the IC_{50} values were calculated as previously described.[29] For detection of inhibition of HIV-1 infection of MT-2 cells using the p24 antigen assay, 1×10^4 MT-2 cells were infected with HIV-1_{IIIB} (100 TCID50) in the presence of LS at graded concentrations, followed by incubation at 37 °C overnight. The culture media was changed, and cells were cultured for 4 days before collection of supernatants for measuring the p24 antigen by ELISA, as described earlier.[30,31]

In Vitro Cytotoxicity of Lignin Sulfate Samples. The in vitro cytotoxicity for MT-2 cells of lignin sulfates was determined in 96-well plates using the XTT dye to measure cell viability in the absence

* Author to whom correspondence should be addressed. Phone: (804) 828-7328. Fax: (804) 827-3664. E-mail: urdesai@vcu.edu.
[†] Virginia Commonwealth University.
[‡] University of Illinois at Chicago.
[§] New York Blood Center.

10.1021/bm0701651 CCC: $37.00
Published on Web 04/17/2007

of virus. A solution of 5% Tritox X-100 (10 mL) was added to the wells corresponding to positive controls (*P*), and 10 mL of medium was added to wells corresponding to negative controls (*N*). The percent cytotoxicity was calculated using the formula $[(E - N)/(P - N)] \times 100$, where *E* represents the experimental data in the presence of lignin sulfates. The concentration corresponding to 50% cytotoxicity (CC_{50}) for MT-2 cells was calculated using the Calcusyn computer program from which the selectivity index ($SI = CC_{50}/IC_{50}$) was calculated.

Molecular Modeling Studies on Heparan Sulfate Disaccharides and Lignin Sulfate Dimers. Structures of LS dimers were built in Sybyl 6.9.2, assigned Gasteiger−Hückel charges and minimized using the Tripos force field at dielectric constant of 80 subject to the gradient termination criterion of 0.01 kcal/mol·Å. The sulfur and oxygen atoms in the sulfate groups were assigned $S.O_2$, $O.CO_2$, and O.3 atom type. A total of 6 $\beta-O-4$- and $\beta-5$-linked lignin dimers containing three sulfate groups each were modeled. The modeling of HS disaccharides followed the protocol used in our earlier report.[32] Briefly, 15 disaccharides, of the naturally occurring 23 disaccharides, containing at least three anionic groups were modeled. The structural differences between these 15 disaccharides are mainly determined by the pattern of sulfation and epimer (IdoA*p*) conformation. The φ_H/ψ_H torsion angles in these disaccharides were obtained from crystal structure studies, as extensively reviewed in our computational study of HS hexasaccharides.[32] Thus, the values were constrained at the average value of 47.5° and 13°, respectively, using a force constant of 0.01 kcal mol^{-1} deg^{-2}. Following minimization, each structure was analyzed for distance between its anionic groups (carboxylates and sulfates). The carbon and sulfur atoms in the carboxylate and sulfate groups, respectively, were used for interanionic distance analysis. Triangular arrays of interanionic distances in LS dimers were prepared and compared to that for HS disaccharides. An LS dimer was considered a mimic of an HS disaccharide if each distance in the triangular array matched within ±1 Å.

Results

Structure of Lignin Sulfate. Lignin is one of the most abundant plant natural products, yet detailed structure of the molecule remains unclear.[25,26] Lignin is a highly heterogeneous polydisperse polymer constituted of phenylpropanoid monomers, which are connected through $\beta-O-4$, $\beta-5$, $\beta-\beta$, or 5−5 linkages (Figure 1). Of these inter-residue linkages, $\beta-O-4$ and $\beta-5$ linkages are reported to be most commonly present. Atmospheric pressure chemical ionization mass spectrometry analysis suggested that our natural product also contained $\beta-O-4$-linked *p*-hydroxycinnamyl alcohol monomers with smaller proportions of $\beta-\beta$-, $\beta-5$-, and 5−5-linked structures.[24] Chemical sulfation of the natural product using triethylamine−sulfur trioxide complex retains these inter-residue linkages, while introducing sulfate groups ($-OSO_3^-$) on the available alcoholic and phenolic −OH groups.[24,33] Thus, chemically sulfated lignin is also a heterogeneous biomacromolecule consisting of a large number of diverse structures, which may be thought of as an LS library. A characteristic feature of this library is the presence of both strongly hydrophilic ($-OSO_3^-$) and strongly hydrophobic (−Ar) groups. In this manner, the LS library is dramatically different from the HS library, which has no aromatic features and minimal levels of hydrophobicity. However, as with all heterogeneous polymers, this library is a double-edged sword. While structural diversity present in the library enhances the probability of discovering biological activity, it also prohibits a definitive assignment of a specific structure(s) as the origin of this activity.

Size Fractionation and Sulfation Level of Lignin Sulfate. Size exclusion chromatography (SEC) of LS indicated polymeric chains with a wide range of molecular weights: 1.5−40 kDa. To gain insight into chain length dependence and elucidate whether smaller LS structures possess antiviral activity, the polymer was fractionated into five fractions using a combination of centrifugal membrane filtration and SEC chromatography.[24] With the use of a calibration curve prepared with polysulfonate standards, the average molecular weight (M_R) of the five fractions were found to be 39.4, 14.9, 5.9, 2.5, and 1.9 kDa. The sulfation level of each fraction was calculated from its elemental composition, especially its sulfur content (∼12% w/w), and found to be nearly identical (not shown). This indicates an average composition of approximately one sulfate group per *p*-hydroxycinnamyl monomer. This level of negative charge density is significantly lower than that of heparin, which typically contains ∼1.8 anionic ($-COO^-$ and $-OSO_3^-$) groups per monomer,[34] while it is equivalent to the average charge density of 1.0−1.4 found in HS.[35,36]

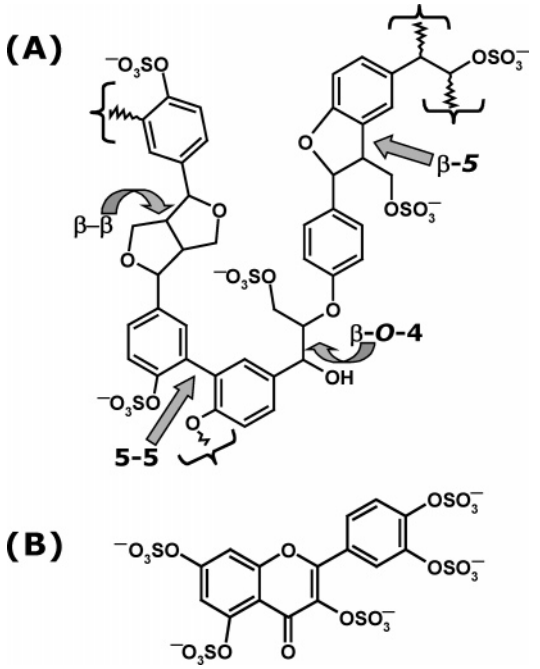

Figure 1. Representation of the structure of lignin sulfate (LS) (A) and morin sulfate (MoS) (B). $\beta-O-4$, $\beta-\beta$, $\beta-5$, and 5−5 in (A) indicate types of intermonomer linkages, while curly brackets show the polymerization points. Positions α, β, 4, and 5, which constitute linkage positions, are marked.

Lignin Sulfate Fractions Inhibit Cellular Entry of HSV. The ability of LS fractions to inhibit entry of HSV-1 and HSV-2 particles was studied in a well-established viral infection assay, in which the internalized viral particle is quantified indirectly through the β-galactosidase activity expressed by its genome.[10,13,27,28] This assay involves the exposure of a constant dose of the virus, mutant strains of HSV-1 and HSV-2 containing the *lacZ* gene, to HeLa cells for 6 h at 37 °C in the presence of sulfated inhibitors at several graded concentrations. Following incubation, the β-galactosidase activity of the internalized virus is measured spectrophotometrically, which is directly proportional to the level of viral particles that have entered the cells.

All five fractions of LS showed a concentration-dependent inhibition of cellular entry of HSV types 1 and 2 (Figure 2). We also tested MoS, a small sulfated organic molecule, which we had synthesized earlier.[33] MoS is a small homogeneous molecule containing five sulfate groups and thus represents a high charge density reference. The response to increasing LS concentration was found to be sigmoidal and when fit to the standard dose−response equation gave the concentration of the inhibitor required for 50% inhibition (IC_{50}) (Table 1). The IC_{50}

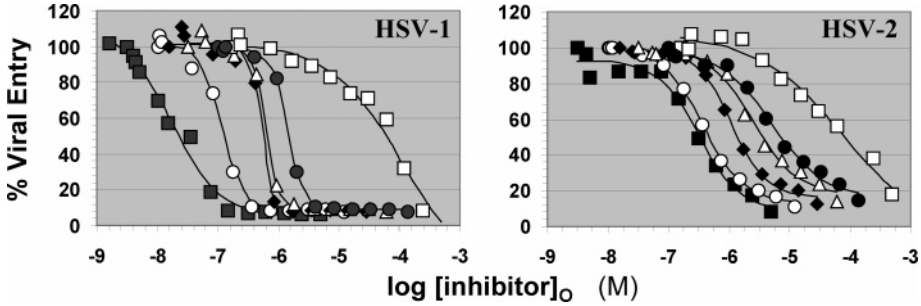

Figure 2. Inhibition of HSV-1 and HSV-2 entry into HeLa cells by lignin sulfate (LS). HeLa cells were exposed to the virus for 6 h at 37 °C in the presence and absence of LS fractions in varying amounts. Following incubation, the cells were solubilized and the initial rate of hydrolysis of the β-galactosidase substrate, ONPG, was monitored spectrophotometrically to determine percent viral entry, as previously described (refs 10, 11, 26, and 27). Labels ■, ○, ◆, Δ, and ●, correspond to LS fractions with M_R values of 39.4, 14.8, 5.9, 2.5, and 1.9 kDa, respectively, while □ corresponds to MoS.

Table 1. Molecular Weight Dependence of IC_{50} Values for LS-Dependent Inhibition of HSV Entry into HeLa Cells

		IC_{50}[a]	
	M_R (kDa)	HSV-1 (μM)	HSV-2 (μM)
LS1	39.4	0.017	0.32
LS2	14.8	0.12	0.40
LS3	5.9	0.53	1.0
LS4	2.5	0.60	2.5
LS5	1.9	1.45	5.0
MoS	0.8	112	79

[a] Values are mean of two experiments.

value for HSV-1 inhibition decreases from 1.45 μM for the smallest LS with M_R of 1.9 kDa to 17 nM for 39.4 kDa LS. In contrast, the IC_{50} value for MoS was found to be 112 μM. Likewise, the IC_{50} values for HSV-2 inhibition were found to be between 0.32 and 5.0 μM for LS fractions, while that for MoS was 79 μM.

Lignin Sulfate Fractions Inhibit HIV-1-Mediated Cell−Cell Fusion. Inhibition of cell fusion activity of HIV-1 was studied by incubating fluorophore-Am-labeled HIV-1_{IIIB}-infected H9 cells with MT-2 cells in the presence and absence of varying concentrations of LS, as described earlier.[30,31,37,38] In this well-established assay, the fluorescence of the infected cells, which fuse with the target cells, is used as the reporter of infectivity. Following incubation for 2 h at 37 °C, the fused and unfused cells were counted in an inverted fluorescence microscope to determine percent inhibition. As the concentration of each LS fraction increased, the fusion of the two types of cells decreased in a sigmoidal manner (not shown), from which the IC_{50} value was calculated (Table 2). The IC_{50} values increase gradually from 60 nM for LS1 to 763 nM for LS5. These values are in the same range as those for the inhibition of cellular entry of HSV-1 (Table 1). As in the HSV study, MoS was found to be a poor inhibitor of HIV-1-mediated cell fusion.

Lignin Sulfate Fractions Inhibit HIV-1. To determine whether LS fractions inhibit HIV-1, we utilized the standard p24 antigen assay.[30,38] Protein p24 is a major internal structural protein of HIV-1, which has been routinely used as a marker of infection. Briefly, MT-2 cells were exposed to a fixed dose of HIV-1_{IIIB} in the presence of increasing concentrations of LS fractions. Following overnight incubation at 37 °C, the culture medium was changed and the cells left undisturbed for 4 days before collection of the supernatant medium for p24 detection by ELISA.[30,37,38] As observed in cell fusion assay, HIV-1 was found to be inhibited by LS fractions (Table 2). The IC_{50} values range from 29 to 400 nM and generally correlate well (1−2-fold difference) with those measured in the cell fusion assay.

Table 2. IC_{50} Values for Inhibition of HIV-1-Mediated Cell Fusion, Entry into MT-2 Cells, and Cytotoxic Effect (CC_{50}) of LS Fractions[a,b]

		IC_{50} (nM)			
	M_R (kDa)	cell fusion	p24[c]	CC_{50} (nM)[a]	selectivity index[d]
LS1	39.4	60	29	603	20.8
LS2	14.8	105	97	1340	13.8
LS3	5.9	246	236	3834	16.2
LS4	2.5	384	400	10280	25.7
LS5	1.9	763	358	10945	30.6
MoS	0.8	>250000	>125000	nd[e]	

[a] CC_{50}: concentration of inhibitor that reduces the number of viable cells by 50% in the absence of infection. [b] Monitored by HIV-1-mediated cell fusion formation between H9/HIV-1_{IIIB} and MT-2 cells (refs 29, 36, and 37). [c] Monitored by production of p24 following infection by laboratory-adapted HIV-1_{IIIB} strain (refs 29, 36, and 37). [d] Ratio of CC_{50} to IC_{50} determined in the p24 assay. [e] Not determined.

Cytotoxic Effect of Lignin Sulfate Fractions. To assess whether the antiviral activities of LS arise from its cytotoxic activity, we measured cell viability on the sixth day without viral exposure in the presence of varying concentrations of LS, as previously described.[30] The cells were exposed to XTT tetrazoline dye, and the concentration of dye internalized by viable cells was measured spectrophotometrically at 450 nm. The concentration corresponding to CC_{50} for MT-2 cells was found to be in the range of 0.6−11 μM, which is nearly 14−31-fold higher than the IC_{50} of LS fractions (Table 2). This suggests a reasonably good SI for sulfated lignin. Interestingly, the cytotoxicity of LS is found to be proportional to the M_R of the polymer and appears to level off for smaller species.

Comparative Molecular Modeling of Lignin Sulfate Dimers and Heparan Sulfate Disaccharides. To determine whether certain LS structures mimic HS sequence(s), we resorted to a comparison of the three-dimensional orientation of sulfate groups by the two strikingly different scaffolds. More specifically, the ability of the LS scaffold to place three sulfate groups in an identical spatial orientation as three anionic groups (carboxylate or sulfate) present in the smallest HS repeat sequence, a disaccharide, was compared using molecular modeling. We hypothesized that LS dimers would mimic HS disaccharides based on their approximately equal size as well as similar negative charge density (~1−1.3 anions per monosaccharide).[35,36]

Of the 23 possible natural HS disaccharides, 15 contain at least 3 anionic groups (Figure 3). Our previous molecular modeling study suggests that HS sequences adopt an average

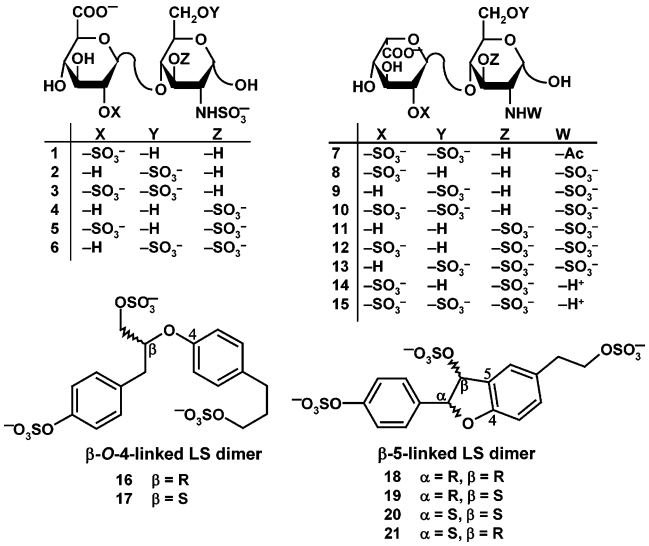

Figure 3. Structures of dimeric units of HS and LS studied for comparative molecular modeling. Six trisulfated $\beta-O-4$- and $\beta-5$-linked LS dimers were compared with 15 HS disaccharides that contain at least three anionic ($-COO^-$ and $-OSO_3^-$) groups.

backbone conformation with similar φ_H/ψ_H torsion angles and the structural differences between the individual sequences are mainly a function of sulfation pattern and uronic acid epimer conformation.[32] Thus, the φ_H/ψ_H angles and $^1C_4/^2S_0$ conformations of IdoA*p* residue were extracted from cocrystal structure of HS sequences and used to construct the 15 disaccharides targeted in this study. Likewise, six different trisulfated LS dimers based on $\beta-O-4$ and $\beta-5$ linkages are possible (Figure 3). These LS dimers were constructed in silico using the small organic molecule builder in Sybyl, and their structures were optimized using standard energy minimization routines. Following the construction of both sets of dimers—HS and LS—interanion distances were calculated. The interanion distance set revealed that selected LS dimers positioned sulfate groups in a manner identical to that possible with certain HS disaccharides. For example, the αR,βS and αS,βR enantiomers of the $\beta-5$-linked LS dimer, i.e., molecules **21** and **19** (Figure 3) were found to mimic HS disaccharides **2** and **1**, respectively. Figure 4 shows the correspondence between the three sulfate groups present in each dimeric pair. Likewise, $\beta-O-4$-linked LS dimers **16** and **17** (Figure 3) were found to mimic HS disaccharides **13** and **5**, respectively (not shown). Yet, not all LS dimers studied were found to mimic HS disaccharides as well as not all HS structures could be mimicked by LS. For example, the αS,βS-linked $\beta-5$ LS dimer **20** did not appear to mimic any of the 15 HS disaccharides. Overall, comparative molecular modeling based on first principles demonstrated that selected LS structures are likely to mimic certain HS sequences.

Discussion

Our serendipitous discovery[24] that LS is an antagonist of HSV-1 led to the reasoning that the biomacromolecule is likely to inhibit other enveloped viruses, e.g., HSV-2 and HIV-1. This expectation was borne out of the possibility that LS, a heterogeneous, polydisperse, sulfated polymer, mimics HS, a major cellular receptor which recognizes viral glycoproteins, including gB, gC, gD of HSV[2,3,5,7−10] and gp120 and Tat of HIV.[1,4,6,11−13]

This work demonstrates that polymeric LS is a reasonably good antagonist of HSV-1, HSV-2, and HIV-1. For the viruses studied, the inhibition was dependent on the molecular weight

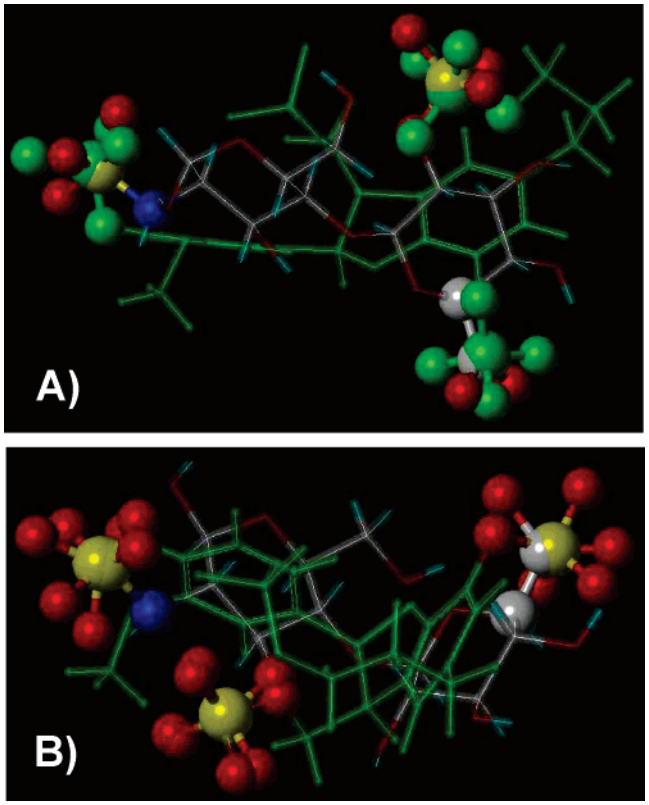

Figure 4. Comparison of three-dimensional orientation of anionic groups of LS dimers **19** and **21** in green sticks (see Figure 3 for structures) with HS disaccharides **1** and **2** in atom-type sticks, respectively; (A) shows a comparison between **21** and **2**, while (B) shows comparison between **19** and **1**. Note the identical orientation of three $-OSO_3^-$ groups in each pair (shown as ball and stick).

of LS with the heaviest chain possessing highest potency. This activity is comparable to the nanomolar activity of soluble HS and heparin.[18] Yet, an interesting observation is that the lighter chains (M_R 1.9 kDa) display significant antagonism, e.g., an IC_{50} value of 1.5 and 5.0 μM against HSV and ~0.36 μM against HIV. Except for the size, the heavier and lighter chains are structurally equivalent.[24] Thus, either the longer chain interacts with additional amino acid residues on the target protein in comparison to the shorter chain or it has a statistical advantage. Studies with more homogeneous species, perhaps synthetic oligomers, may clarify this feature.

The work reveals additional interesting aspects of viral antagonism. First, MoS containing five sulfate groups in its small size (0.8 kDa, Figure 1) is a 16−78-fold weaker inhibitor of HSV entry and at least 300-fold weaker inhibitor of HIV entry than the smallest LS (M_R 1.9 kDa). The presence of five sulfate groups in MoS introduces massive anionic character in the molecule. In comparison, LS has much lower charge density. Thus, it is likely that the activity of LS arises from its structural features, rather than from the general recognition of its few sulfate groups. Second, the IC_{50} values decrease for both HSV-1 and HSV-2 as the M_R of LS samples increase (Table 1). However, the decrease is not parallel (not shown). For example, the potency for HSV-1 inhibition increases ~85-fold with the M_R, while only a 16-fold increase in potency was found for HSV-2. This indicates a difference in the activity of LS against the two viruses, an observation also found to be true with heparin.[39]

The heterogeneous and polydisperse nature of LS implies a large number of distinct structures in these preparations. The M_R of LS monomers is ~200 Da. Thus, an average 1.9 kDa

chain is expected to consist of four to five dimers. The possibility of several inter-residue linkages, $\beta-O-4$, $\beta-5$, $\beta-\beta$, and 5−5, in these chains introduce significant complexity in identification of discrete structures responsible for antiviral activity. It may be possible to identify potent sequences in this heterogeneous mixture using a combination of affinity and ion-exchange chromatographies; however, the target HSV/HIV proteins remain unknown at present resulting in considerable ambiguity. Another approach that may yield useful sequence information is modeling. Comparative molecular modeling of a limited set of structures shows that certain LS sequences may mimic selected HS sequences by orienting appropriate sulfate groups in a nearly identical manner (Figure 4). These results indicate that LS may be a reasonably good mimic of HS, although high-affinity sequence information is still a matter of future work. A specific advantage with the LS structure, in comparison with the HS scaffold, is that it is an aromatic, hydrophobic skeleton, which is readily amenable to chemo−enzymatic synthetic approach and structural modification.

Acknowledgment. This work was supported by the NIH (RO1 HL069975 and R41 HL081972) and AHA−National Center (EIA 0640053N).

References and Notes

(1) Ugolini, S.; Mondor, I.; Sattentau, Q. J. *Trends Microbiol.* **1999**, *7*, 144−149.
(2) Spear, P. G.; Eisenberg, R. J.; Cohen, G. H. *Virology* **2000**, *275*, 1−8.
(3) Shukla, D.; Spear, P. G. *J. Clin. Invest.* **2001**, *108*, 503−510.
(4) Gallay, P. *Microbes Infect.* **2004**, *6*, 617−622.
(5) Spear, P. G. *Cell. Microbiol.* **2004**, *6*, 401−410.
(6) Fittipaldi, A.; Giacca, M. *Adv. Drug Delivery Rev.* **2005**, *57*, 597−608.
(7) Herold, B. C.; Visalli, R. J.; Susmarski, N.; Brandt, C. R.; Spear, P. G. *J. Gen. Virol.* **1994**, *75*, 1211−1222.
(8) Shukla, D.; Liu, J.; Blaiklock, P.; Shworak, N. W.; Bai, X.; Esko, J. D.; Cohen, G. H.; Eisenberg, R. J.; Rosenberg, R. D.; Spear, P. G. *Cell* **1999**, *99*, 13−22.
(9) Cheshenko, N.; Herold, B. C. *J. Gen. Virol.* **2002**, *83*, 2247−2255.
(10) Tiwari, V.; Clement, C.; Duncan, M. B.; Chen, J.; Liu, J.; Shukla, D. *J. Gen. Virol.* **2004**, *85*, 805−809.
(11) Zhang, Y.-J.; Hatziioannou, T.; Zang, T.; Braaten, D.; Luban, J.; Goff, S. P.; Bieniasz, P. D. *J. Virol.* **2002**, *76*, 6332−6342.
(12) Argyris, E. G.; Kulkosky, J.; Meyer, M. E.; Xu, Y.; Mukhtar, M.; Pomerantz, R. J.; Williams, K. J. *Virology* **2004**, *330*, 481−486.
(13) Vives, R. R.; Imberty, A.; Sattentau, Q. J.; Lortat-Jacob, H. *J. Biol. Chem.* **2005**, *280*, 21353−21357.
(14) Esko, J. D.; Lindahl, U. *J. Clin. Invest.* **2001**, *108*, 169−173.
(15) Rabenstein, D. L. *Nat. Prod. Rep.* **2002**, *19*, 312−331.
(16) Liu, J.; Shriver, Z.; Pope, R. M.; Thorp, S. C.; Duncan, M. B.; Copeland, R. J.; Raska, C. S.; Yoshida, K.; Eisenberg, R. J.; Cohen, G.; Linhardt, R. J.; Sasisekharan, R. *J. Biol. Chem.* **2002**, *277*, 33456−33467.
(17) Nishimura, S. I.; Kai, H.; Shinada, K.; Yoshida, T.; Tokura, S.; Kurita, K.; Nakashima, H.; Yamamoto, N.; Uryu, T. *Carbohydr. Res.* **1998**, *306*, 427−433.
(18) Witvrouw, M.; De Clercq, E. *Gen. Pharmacol.* **1997**, *29*, 497−511.
(19) Ponce, N. M.; Pujol, C. A.; Damonte, E. B.; Flores, M. L.; Stortz, C. A. *Carbohydr. Res.* **2003**, *338*, 153−165.
(20) Viveros-Rogel, M.; Soto-Ramirez, L.; Chaturvedi, P.; Newburg, D. S.; Ruiz-Palacios, G. M. *Adv. Exp. Med. Biol.* **2004**, *554*, 481−487.
(21) Nyberg, K.; Ekblad, M.; Bergstrom, T.; Freeman, C.; Parish, C. R.; Ferro, V.; Trybala, E. *Antiviral Res.* **2004**, *63*, 15−24.
(22) Damonte, E. B.; Matulewicz, M. C.; Cerezo, A. S. *Curr. Med. Chem.* **2004**, *11*, 2399−2419.
(23) Urbinati, C.; Bugatti, A.; Oreste, P.; Zoppetti, G.; Waltenberger, J.; Mitola, S.; Ribatti, D.; Presta, M.; Rusnati, M. *FEBS Lett.* **2004**, *568*, 171−177.
(24) Raghuraman, A.; Tiwari, V.; Thakkar, J. N.; Gunnarsson, G. T.; Shukla, D.; Hindle, M.; Desai, U. R. *Biomacromolecules* **2005**, *6*, 2822−2832.
(25) Reale, S.; Di Tullio, A.; Spreti, N.; De Angelis, F. *Mass Spectrom. Rev.* **2004**, *23*, 87−126.
(26) Davin, L. B.; Lewis, N. G. *Curr. Opin. Biotechnol.* **2005**, *16*, 407−415.
(27) Montgomery, R. I.; Warner, M. S.; Lum, B. J.; Spear, P. G. *Cell* **1996**, *87*, 427−436.
(28) Warner, M. S.; Geraghty, R. J.; Martinez, W. M.; Montgomery, R. I.; Whitbeck, J. C.; Xu, R.; Eisenberg, R. J.; Cohen, G. H.; Spear, P. G. *Virology* **1998**, *246*, 179−189.
(29) Jiang, S.; Lin, K.; Strick, N.; Neurath, A. R. *Biochem. Biophys. Res. Commun.* **1993**, *195*, 533−538.
(30) Debnath, A. K.; Radigan, L.; Jiang, S. *J. Med. Chem.* **1999**, *42*, 3203−3209.
(31) Jiang, S.; Lin, K.; Lu, M. *J. Virol.* **1998**, *72*, 10213−10217.
(32) Raghuraman, A.; Mosier, P. D.; Desai, U. R. *J. Med. Chem.* **2006**, *49*, 3553−3562.
(33) Gunnarsson, G. T.; Desai, U. R. *Bioorg. Med. Chem. Lett.* **2003**, *13*, 579−583.
(34) Vongchan, P.; Warda, M.; Toyoda, H.; Toida, T.; Marks, M.; Linhardt, R. J. *Biochim. Biophys. Acta* **2005**, *1721*, 1−8.
(35) Warda, M.; Gouda, E. M.; Toida, T.; Chi, L.; Linhardt, R. J. *Comp. Biochem. Physiol., B* **2003**, *136*, 357−365.
(36) Warda, M.; Linhardt, R. J. *Comp. Biochem. Physiol., B* **2006**, *143*, 37−43.
(37) Jiang, S.; Lin, K.; Zhang, L.; Debnath, A. K. *J. Virol. Methods* **1999**, *80*, 85−96.
(38) Naicker, K. P.; Jiang, S.; Lu, H.; Ni, J.; Boyer-Chatenet, L.; Wang, L.-X.; Debnath, A. K. *Bioorg. Med. Chem.* **2004**, *12*, 1215−1220.
(39) Trybala, E.; Liljeqvist, J.-A.; Svennerholm, B.; Bergstrom, T. *J. Virol.* **2000**, *74*, 9106−9114.

BM0701651